Focus Expansion in Plant Disease. II: Realistic Parameter-Sparse Models

F. van den Bosch, J. C. Zadoks, and J. A. J. Metz

First and third authors, Institute of Theoretical Biology, State University of Leiden, Groenhovenstraat 5, 2311 BT Leiden, The Netherlands; second author, Laboratory of Phytopathology, Agricultural University, Binnenhaven 9, 6709 PD Wageningen, The Netherlands.

We are grateful to two anonymous referees whose criticisms greatly improved the text. We wish to thank Y. Zitman for typing the manuscript and G. P. G. Hock for drawing the figures.

Accepted for publication 8 September 1986.

ABSTRACT

van den Bosch, F., Zadoks, J. C., and Metz, J. A. J. 1988. Focus expansion in plant disease. II: Realistic parameter-sparse models. Phytopathology 78:59-64.

In a previous paper, a model was presented applicable to the expansion of plant disease foci. The model permits calculating the velocity of focus expansion and the slope of the focal front in a few seconds of microcomputer time. In this paper, a parameter-sparse and yet sufficiently flexible subclass of models is considered that can easily be adapted to various pathosystems. A mechanistic submodel is introduced for the dispersal of infectious units, based on turbulent diffusion inside the canopy and random interception of infectious units by host plants. It describes the contact distribution, a concept analogous to the primary gradient of a focus. The production of infectious units as a function of the time after infection is described by a shifted gamma density. These submodels are shown to fit some published data sets. With the resulting model, the effect of various parameters of contact distribution and time kernel submodels on the velocity of the expanding focus and the slope of its front was investigated.

Additional key words: contact distribution, epidemic wave, gross reproduction, spore dispersal, time kernel.

In a previous paper (2), a general model for the spatial spread of an infectious disease was discussed, following Diekmann (4,5) and Thieme (19,20). That model, which is a spatial variant of the Kermack & McKendrick model (9,16), can be applied to the development of foci in agricultural pathosystems. After a phase of focus buildup, a focus initiated by a single infectious unit will expand radially in wavelike fashion (19). The velocity of the wave will approach a constant value, c, called the asymptotic wave velocity. The *front* of the wave, expressed in terms of density of diseased individuals, has an exponential shape characterized by a shape parameter λ.

Two equations were derived to calculate c and λ from three features of the pathosystem: the contact distribution ($D(\vec{x})$), characterizing inoculum dispersal; the normalized time kernel ($i(\tau)$), describing the relative rate of inoculum production; and the gross reproduction (γS_0), which is the number of daughter lesions per mother lesion in an otherwise uninfected field, including multiple infections.

As an example, wave velocities were calculated for a time kernel with fixed latency period (p), fixed infectious period (i), and constant spore production during the infectious period. In other words, the time kernel was a block function. The contact distribution was assumed to be Gaussian. This example is a spatial variant of Vanderplank's (23) equation, introduced in a simulation context by Kampmeijer and Zadoks (7). In reality, inoculum production is not constant throughout the infectious period. It starts slowly, reaches a peak, and tapers off to zero (5,8,11,12,15). In addition, measured contact distributions are more peaked than the Gaussian distribution (13,14,22,25).

Obviously, a more realistic model is needed, as Minogue and Fry (17) also stated. Therefore, a family of models will be treated that is both sufficiently parameter-sparse to be manageable and sufficiently flexible to cover many real-life situations. For the contact distribution, a mechanistic submodel will be introduced based on random movement of infectious units and random interception by host individuals. For the time kernel, a descriptive submodel will be introduced using a fixed latency period (p) and a gamma density to describe spore production during the infectious period. The effect of various parameters in the submodels on the wave velocity, c, and the shape parameter, λ, will be investigated. Symbols are explained in Table 1.

CONTACT DISTRIBUTION

In dense agricultural crops such as rice or wheat, the movement of infectious units is the result of air turbulence within the canopy boundary layer. It is assumed that all infectious units are equally mobile and move at random. Therefore, the distribution of those units that are not yet trapped follows a Gaussian density with a variance that increases linearly with time,

TABLE 1. List of symbols

Symbol	Explanation	Dimension
β	Constant of gamma density	$[T^{-1}]$
c	Asymptotic wave velocity	$[LT^{-1}]$
γS_0	Gross reproduction	[1]
$\Gamma(n)$	Gamma function	[1]
$D(x_1,x_2)$	Contact distribution	$[L^{-2}]$
$D^0(x)$	Probability distribution of daughter lesions on transect through source	$[L^{-1}]$
$\tilde{D}(x)$	Marginal distribution of contact distribution	$[L^{-1}]$
δ	Probability of interception	$[T^{-1}]$
$i(\tau)$	Time kernel	$[T^{-1}]$
i	Infectious period	[T]
λ	Shape parameter of wave front	$[L^{-1}]$
μ_i	Mean of infectious period	[T]
n	Constant of gamma density	[1]
ν^2	Variance of time kernel	$[T^2]$
p	Latency period	[T]
σ_1^2	Variance of $D^0(x)$	$[L^2]$
σ_2^2	Variance of $\tilde{D}(x)$	$[L^2]$
ω	Diffusion constant	$[L^2T^{-1}]$

$$\frac{1}{2\pi\omega\tau} \exp\left[-\frac{x_1^2 + x_2^2}{2\omega\tau}\right], \qquad (2.1)$$

where ω is the rate of increase of the variance. Infectious units are intercepted by suscepts and nonsuscepts alike. We assume that this happens with a probability δ per unit of time. Therefore, the time to trapping is exponentially distributed with rate parameter δ,

$$\delta \exp\left[-\delta\tau\right]. \qquad (2.2)$$

(In general, the mean free lifetime of an infectious unit (δ^{-1}) will be short relative to the infectious period. This enables us to describe disease transfer in terms of two separate functions, a contact distribution and a time kernel.)

The final distribution of trapped spores, the contact distribution, is given by multiplying equation 2.1 with equation 2.2 and integrating with respect to τ. Finally, putting $\tau' = \omega\tau$, and immediately dropping the suffix node again, we arrive at:

$$D(x_1, x_2) = \frac{1}{2\pi\omega/\delta} \int_0^\infty \frac{1}{\tau} \exp\left[-\tau - \frac{x_1^2 + x_2^2}{2\tau\omega/\delta}\right] d\tau. \qquad (2.3)$$

This so-called Bessel distribution was first derived by Williams (27) and Broadbent and Kendall (3) in a different but comparable context. Usually data are given as measurements along a transect through the point of inoculation. The distribution along such a transect (corresponding to the distribution of one coordinate, x_1, conditional on the other coordinate, x_2, being zero) is:

$$D^0(x_1) = \frac{1}{2\pi\sigma_1} \int_0^\infty \frac{1}{\tau} \exp\left[-\tau - \frac{1}{2\sigma_1^2}\frac{x_1^2}{\tau}\right] d\tau \qquad (2.4)$$

where $\sigma_1^2 = \omega/2\delta$ is the variance of D^0. Note that $D^0(x_1)$ is here a one-variable function. The Bessel distribution is more peaked than the Gaussian distribution (Fig. 1).

The marginal distribution, derived from equation 2.3 using equation 3.1 from (2), which is needed to calculate c and λ (2), is the double exponential distribution:

$$\tilde{D}(x_1) = \tfrac{1}{2} \sqrt{2}\frac{1}{\sigma_2} \exp\left[-\sqrt{2}\frac{1}{\sigma_1}|x_1|\right] \qquad (2.5)$$

where σ_2^2 equals the variance of $\tilde{D}(x_1)$ and σ_1 and σ_2 are related by

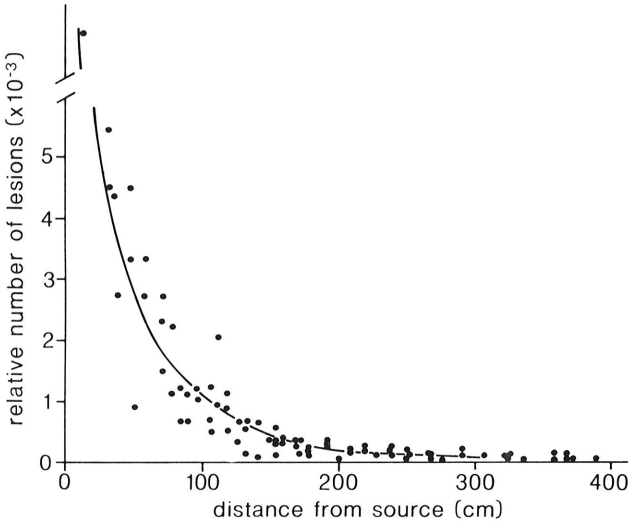

Fig. 1. Contact distribution of rice blast (*Pyricularia oryzae*) on rice (dots). Data from MacKenzie (14). Solid line is Bessel distribution (Eq. 2.1).

$$\sigma_1^2 = 2\,\sigma_2^2. \qquad (2.6)$$

The contact distribution can be determined by counting daughter lesions at various distances from a mother lesion (or a group of closely packed mother lesions taken as a point source) before the granddaughter lesions become apparent. If a point source is used, the density of daughter lesions on a transect through the source follows the Bessel distribution (Eq. 2.4). If a line source is used, the density of daughter lesions along a transect perpendicular to it follows the double-exponential distribution (Eq. 2.5).

In Figure 1, data on rice blast (*Pyricularia oryzae* (Cav.)) from MacKenzie and Villareal (13,14) are shown together with a Bessel distribution fitted by eye. To this end, various values of the parameter σ_1 were used in conjunction with tables (1) until a reasonable value was found.

TIME KERNEL

For the time kernel, recourse is taken to a descriptive model. The submodel should describe a latency period, p, and a smooth and flexible, humplike inoculum production curve covering the infectious period. The so-called shifted gamma density satisfies these demands:

$$i(\tau) = \begin{cases} 0 & \text{if } \tau < p \\ \dfrac{\beta(\beta(\tau - p))^{n-1} \exp\left(-\beta(\tau - p)\right)}{\Gamma(n)} & \text{if } \tau > p. \end{cases} \qquad (3.1)$$

$\Gamma(n)$ is the Gamma function, tabulated in several textbooks (e.g., [1]); n and β are constants. The mean of the time kernel is $p + \mu_i$, where μ_i is the mean time required to produce a randomly selected spore after the latency period, $\mu_i = n/\beta$. The variance, ν^2, of the time kernel equals n/β^2.

Measurements of the latency period and the inoculum production during the infectious period are available from the literature (5,8,11,15,27). Figure 2 shows examples of Gamma distributions eye-fitted to published data. Evidently, equation 3.1 provides a fair description of the time kernel.

WAVE VELOCITY AND SHAPE OF THE WAVE FRONT

The shape of the epidemic front (3,4,19,20) is described by the equation:

$$S_0 - S(t, x) \propto \exp \lambda\,(ct - x_1) \qquad (4.1)$$

where $S_0 - S(t, x)$ is the density of victims at time t and position x, c is the asymptotic wave velocity, and λ is the shape parameter. For an explanation see van den Bosch et al (21). Both c and λ can be calculated (21). Technical details are given in an appendix to this paper.

The parameters of the model can be taken together in dimensionless (also called scaled) parameters (see the appendix):

$$c^* = c\,\mu_i/\sigma_2 \quad [LT^{-1}]\cdot[T]/[L] = [1] \qquad (4.2.a)$$

$$\lambda^* = \lambda\,\sigma_2 \quad [L^{-1}]\cdot[L] = [1] \qquad (4.2.b)$$

$$p^* = p/\mu_i \quad [T]/[T] = [1] \qquad (4.2.c)$$

$$\nu^* = \nu/\mu_i \quad [T]/[T] = [1]. \qquad (4.2.d)$$

In statistical literature, ν/μ_i is called the coefficient of variation. Figure 3 depicts the dependence of the scaled wave velocity and the scaled shape parameter on the gross reproduction, γS_0, and the coefficient of variation, for various values of the scaled latency

period. The dependence of the scaled wave velocity on the scaled latency period is shown in more detail in Figure 4. When, for example, the scaled wave velocity matching a certain γS_0 and ν/μ_i is found in the graph, c can be calculated from $c = c^* \sigma_2/\mu_i$.

The larger the gross reproduction, the larger is c, an effect that can be understood intuitively. Except for γS_0 near unity, c increases nearly logarithmically with γS_0. This can be explained by the following argument. Consider the effect of a line source parallel to the front of the wave. The number of new victims (daughter lesions) per unit of distance (perpendicular to the line source) at a distance x_1 from the source is

$$\gamma S_0 \, \tilde{D}(x_1) = \gamma S_0 \, \tfrac{1}{2}\sqrt{2} \, \frac{1}{\sigma_2} \, \exp\left[-\sqrt{2} \, \frac{1}{\sigma_2} \, |x_1|\right].$$

As a measure of the effect of a distant source, consider the effective distance beyond which the number of daughter lesions per unit of distance decreases below a value K.

$$\gamma S_0 \, \tilde{D}(x_{\text{eff}}) = \mathrm{K} \leftrightarrow x_{\text{eff}} = \tfrac{1}{2}\sqrt{2} \ln \left(\frac{\gamma S_0}{\mathrm{K}} \, \tfrac{1}{2}\sqrt{2} \right). \quad (4.3)$$

The effective distance, which is a measure of the distance covered by one generation, increases logarithmically with γS_0. In this light a logarithmic dependence of c on γS_0 is to be expected.

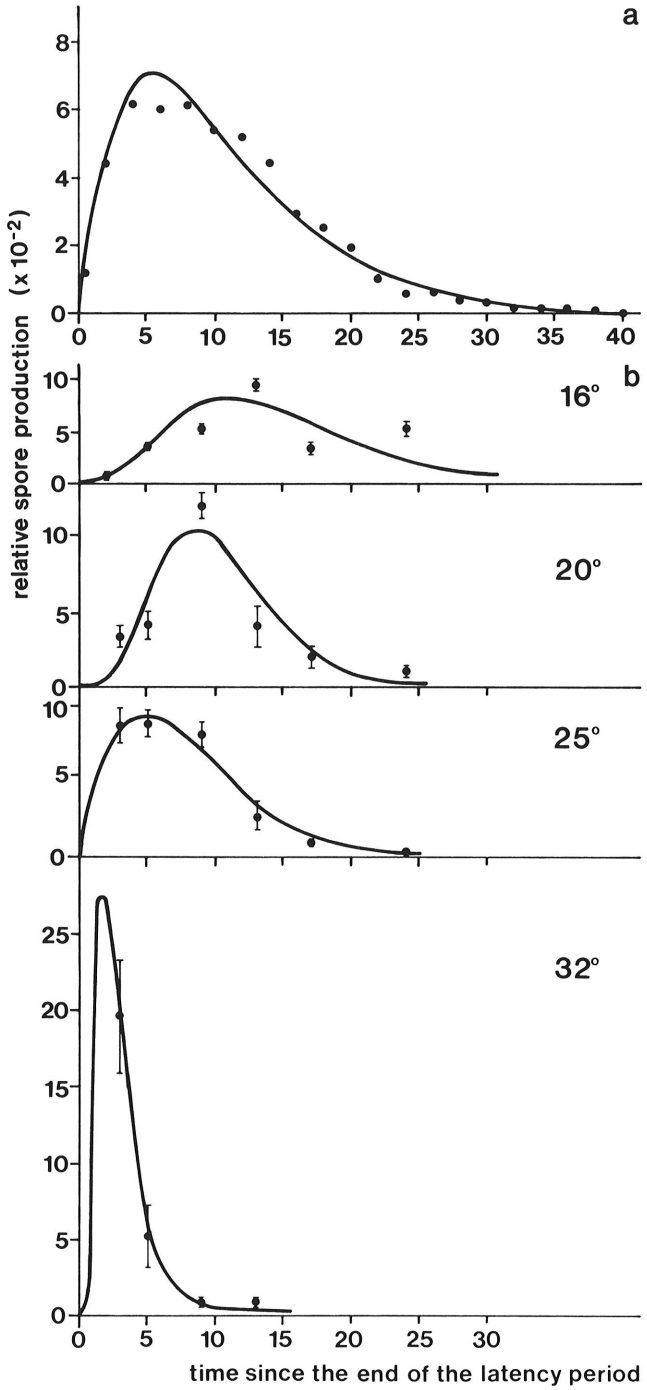

Fig. 2. Observed time kernels (dots). Solid lines are delayed Gamma densities (Eq. 3.2). **A,** Brown rust (*Puccinia recondita*) on wheat seedlings. Data from Mehta and Zadoks (16). **B,** Rice blast (*Pyricularia oryzae*) on rice at various temperatures (°C). Data from Kato and Kozaka (9).

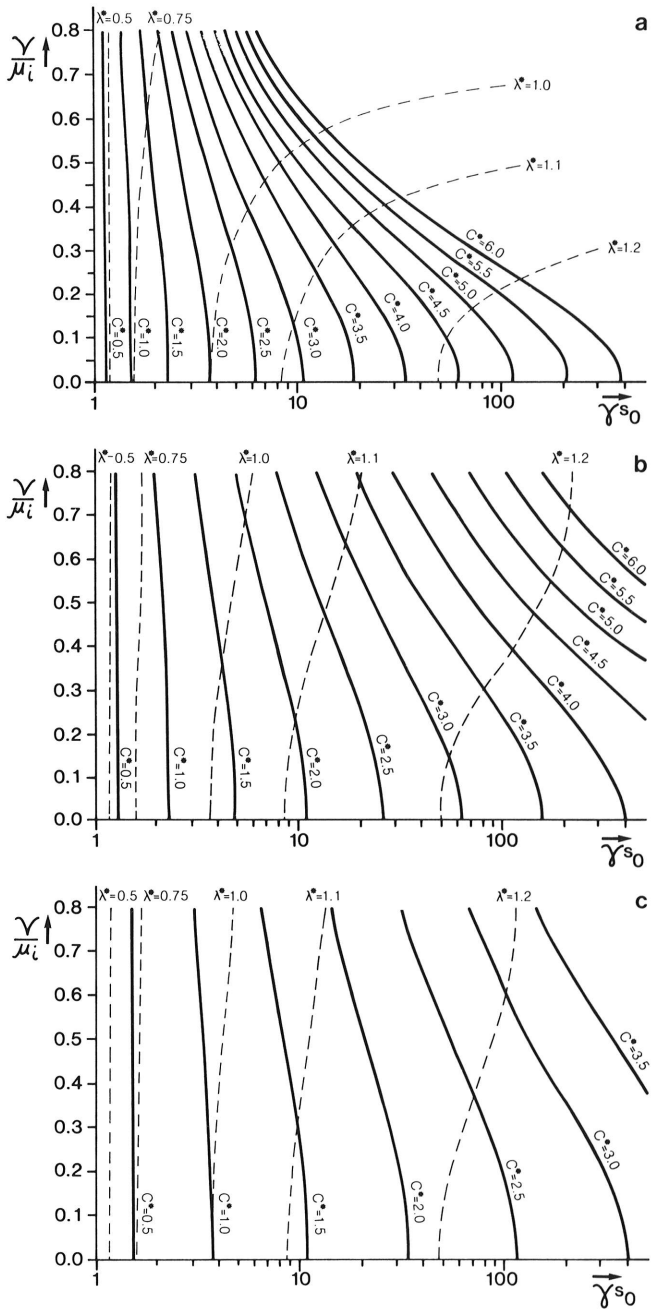

Fig. 3. Asymptotic wave velocity (c^*) and wave-front slope parameter (λ^*) as function of gross reproduction (γS_0) and variation coefficient of infectious period. Solid lines: $c^* = c\mu_i/\sigma_2$. Broken lines: $\lambda^* = \lambda\sigma_2$. **A,** $p/\mu_i = 0.0$; **B,** $p/\mu_i = 0.5$; **C,** $p/\mu_i = 1.0$.

Contrary to the opinion of Vanderplank (24) and MacKenzie (13), but consistent with the results of Minogue and Fry (17), Figure 3 shows that λ decreases with decreasing γS_0. Minogue and Fry (17) argue that this flattening is somehow related to the age distribution of the lesions, but the relationship is not clear. Our results do not yet give more insight into this problem, and further research is needed.

The contact distribution is characterized by one parameter, σ^2. From equation 4.2.a it is seen that the wave velocity increases linearly with σ, as found by Minogue and Fry (17). When the diffusion constant ω increases or when the chance of interception per unit of time, δ, decreases, the infectious units will disperse over larger distances; σ will be larger and, consequently, c will be larger.

From the system of equations in the appendix it can be seen that $\lambda^* = \lambda\sigma \leqslant \sqrt{2}$. No wave front can be steeper than $\exp((-\sqrt{2}/\sigma)x)$, which is the slope of the contact distribution. The shape parameter (λ) depends inversely on the variance of the contact distribution. When σ^2 increases, the contact distribution flattens and the slope of the front decreases. The existence of such a limit is a peculiarity of the exponential and some other contact distributions. If the contact distribution is, for example, Gaussian there is no such restriction on the steepness of the wave front.

The time kernel is based on three parameters, so that relations become rather complex. Figures 3 and 4 show that the latency period p has a marked influence on the wave velocity, as Minogue and Fry (17) also found. Long latency periods produce, as is intuitively understood, low wave velocities, but the relationship is nonlinear.

An increase of the variance of the infectious period (ν_i^2) at a fixed mean (μ_i) causes an increase in wave velocity. A decrease of the mean at fixed variance has the same effect (Fig. 3). As Figure 5 shows, both the increase of the variance and the decrease of the mean result in higher production of inoculum at the beginning of the infectious period. The concomitant lower rate of inoculum production in a later stage of the infectious period has less effect, as the earliest inoculum yields "interest" soonest.

With small ν^2, the slope of the wave front does not depend on latency period p, whereas the wave velocity does. If ν^2, γS_0, and σ are kept constant and $p + \mu_i$ is doubled, the wave velocity is halved; but as the reproduction time is doubled, the wave travels the same distance *per generation* in both cases and the shape of the wave front remains unchanged.

DISCUSSION

In phytopathological literature, it is customary to describe the primary gradient, a concept analogous to contact distribution, by simple equations such as those introduced by Gregory (6) and Kiyosawa and Shiyomi (10). These models lack a mechanistic basis, in contrast to dynamic simulation models describing the dispersal of inoculum within a canopy (18). Such simulation models often are too complex and time-consuming for studying spatial spread of epidemics, and they are not well suited for studying the relationships between model parameters. The Bessel distribution introduced here tries to strike a balance. It is mechanistic, simple, and explicit. At first sight its fit to empirical data seems to be at least as good as the fit of the Gregory or Kiyosawa and Shiyomi model.

Many phytopathological models for epidemic spread use a time kernel, implicit in the Vanderplank (23) equation, with fixed latency period, fixed infectious period, and constant inoculum production rate. Experimental data indicate that such models are too simple. Since the Diekmann and Thieme model allows any time kernel, we introduced the shifted Gamma density as a flexible description of the time kernel that is adequate for practical applications.

The relationship between the asymptotic wave velocity c, the shape parameter of the wave front λ, and various model parameters was studied in this paper, and results were interpreted intuitively. Though the spatial distribution of disease can be understood better by applying the present model, it does not yet tell the whole story. Every parameter is a function of environmental factors, as, for example, the temperature dependence of the latency period. Eventually, such relationships can be incorporated into the model so that the effect of temperature on c and λ can be studied.

Our efforts show that the Diekmann and Thieme model can be

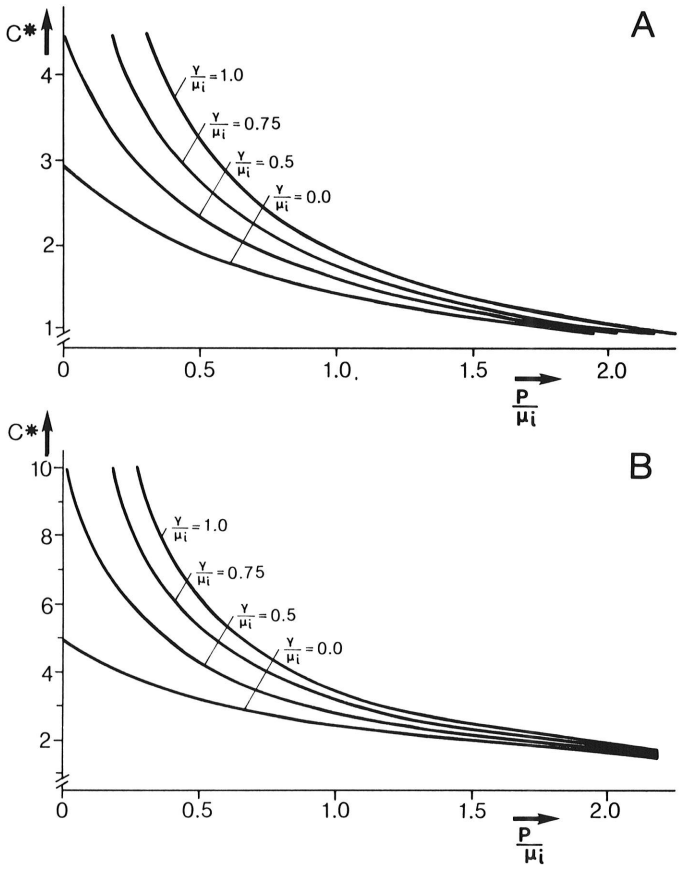

Fig. 4. Dependence of wave velocity ($c^* = c\mu_i/\sigma_2$) on latency period (p/μ_i) for various values of $\nu^* = \nu/\mu_i$. **A**, $\gamma S_0 = 10$; **B**, $\gamma S_0 = 100$.

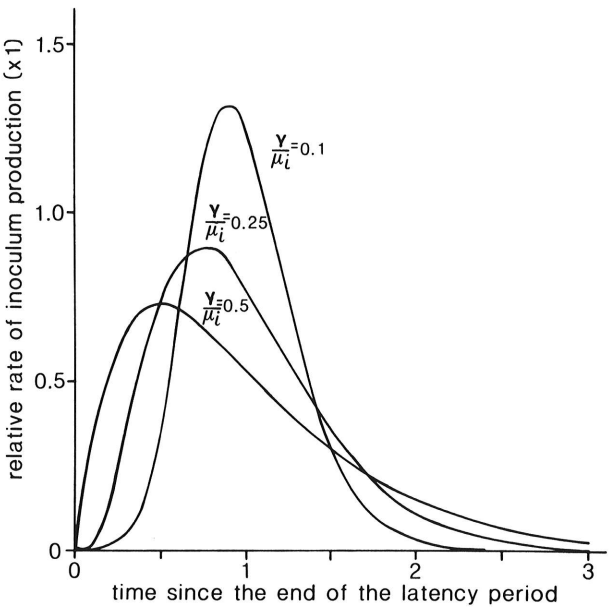

Fig. 5. Shape of Gamma distribution at different values of coefficient of variation (ν/μ_i).

adapted to plant/pathogen systems in a reasonably simple manner. All necessary variables and functions can be measured. In a third paper we shall compare the performance of the model with experimental data.

APPENDIX

The asymptotic wave speed, c, and the wave slope parameter, λ, are the solutions of the system in equation 3.2 with equations 3.3 and 3.4 in van den Bosch et al (21). For the time kernel (Eq. 3.1) and the contact distribution (Eq. 2.5) introduced in this paper, we find:

$$\int_{-\infty}^{\infty} e^{-\lambda x}\,\tilde{D}(x)dx = \tfrac{1}{2}\sqrt{2}\,(1/\sigma_2)\int_{-\infty}^{\infty} e^{-(\lambda x+\sqrt{2}(1/\sigma_2)|x|)}\,dx$$
$$= \tfrac{1}{2}\sqrt{2}\,(1/\sigma_2)\left\{\int_{-\infty}^{0} e^{+(\sqrt{2}(1/\sigma_2)-\lambda)x}\,dx + \int_{0}^{\infty} e^{-(\lambda+\sqrt{2}(1/\sigma_2)x}\,dx\right\}$$

$$= \frac{1}{1-\tfrac{1}{2}(\lambda\sigma_2)^2}$$

(note that $\lambda < \sqrt{2}/\sigma_2$ because otherwise the integral on the left is divergent) and

$$\int_{0}^{\infty} e^{-\lambda c\tau}\,i(\tau)d\tau = \frac{\beta^n}{\Gamma(n)}\int_{p}^{\infty} e^{-\lambda c\tau}(\tau-p)^{n-1}\exp(-\beta(\tau-p))d\tau$$

$$\frac{\beta^n}{\Gamma(n)}\,e^{-\lambda cp}\int_{0}^{\infty} e^{-(\lambda c+\beta)\tau'}(\tau')^{n-1}\,d\tau' = e^{-\lambda cp}\left[\frac{1}{1+\frac{\lambda c}{\beta}}\right]^n$$

(see, e.g., Abramowitz and Stegun [1]). Introduce the scaled parameters

$$\lambda^* = \lambda\sigma_2,\ c^* = c\mu_i/\sigma_2 = cn/\beta\sigma_2,\ p^* = p/\mu_i = p\beta/n,\ \alpha^* = (\mu_i/\nu)^2 = \beta^2.$$

Substitution in equation 3.4 from van den Bosch et al (21) and dropping the asterisks gives

$$L(c,\lambda) = \gamma S_0\ \frac{1}{1-\tfrac{1}{2}\lambda^2}\left[\frac{1}{1+\frac{c\lambda}{\alpha}}\right]^{\alpha} e^{-\lambda cp}.$$

Therefore the system in equation 3.2 in van den Bosch et al (21) becomes

$$\begin{cases} \ln\gamma S_0 - \ln(1-\tfrac{1}{2}\lambda^2) - \lambda cp - \alpha\ln(1+\frac{c\lambda}{\alpha}) = 0, & \text{(A.1.a)} \\ \dfrac{\lambda}{1-\tfrac{1}{2}\lambda^2} - cp - \dfrac{c}{\frac{c\lambda}{\alpha}+1} = 0. & \text{(A.1.b)} \end{cases}$$

(Note that $1-\tfrac{1}{2}\lambda^2$ has to be larger than zero.)

To calculate the lines of equal wave velocity (c^*) of Figure 3 we rewrite equation (A.1.b) as

$$\lambda^3\left\{\tfrac{1}{2}\frac{c^2}{\alpha}p\right\} + \lambda^2\left\{\frac{c}{\alpha} + \tfrac{1}{2}cp + \tfrac{1}{2}c\right\}$$
$$+\lambda\left\{1-\frac{c^2}{\alpha}p\right\} - \left\{cp + c\right\} = 0.$$

For chosen values of c, α, and p, λ can be solved numerically using Newton-iteration. γS_0 is then found from equation A.1.a.

The lines of equal λ of Figure 3 were calculated by solving equation A.1.b for c.

$$c_{\pm} = \frac{-b \pm \sqrt{b^2-4ad}}{2a},$$

where

$$a = \frac{\lambda p}{\alpha}(\tfrac{1}{2}\lambda^2 - 1),\quad b = \lambda^2\left(\frac{1}{\alpha} + \tfrac{1}{2}p + \tfrac{1}{2}\right),\quad d = \lambda.$$

Since $a < 0$, only c_- is positive. γS_0 is found by substituting c_- in equation A.1.a.

To calculate Figure 4, we first multiplied equation A.1.b with λ and subtracted equation A.1.a, giving

$$\ln\gamma S_0 - \ln(1-\tfrac{1}{2}\lambda^2) - \alpha\ln\left(\frac{c\lambda}{\alpha}+1\right) - \frac{\lambda^2}{1-\tfrac{1}{2}\lambda^2} + \frac{c\lambda}{\frac{c\lambda}{\alpha}+1} = 0.$$

For fixed c, γS_0, and α, λ can again be calculated numerically using Newton-iteration. p is found then from:

$$p = \frac{\lambda}{c(1-\tfrac{1}{2}\lambda^2)} - \frac{1}{\frac{c\lambda}{\alpha}+1}.$$

LITERATURE CITED

1. Abramowitz, M., and Stegun, I. A. 1964. Handbook of mathematical functions with formulas, graphs and mathematical tables. Nat. Bur. Stand. Appl. Math. Ser. 55.
2. Broadbent, S. R., and Kendall, D. G. 1953. The random walk of *Trichostrongylus retortaeformis*. Biometrika 9:460-465.
3. Diekmann, O. 1978. Thresholds and travelling waves for the geographical spread of infection. J. Math. Biol. 6:109-130.
4. Diekmann, O. 1979. Run for your life. A note on the asymptotic speed of propagation of an epidemic. J. Differ. Equations 33:58-73.
5. Eyal, Z., and Peterson, J. L. 1967. Uredospore production of five races of *Puccinia recondita* Rob. ex Desm. as affected by light and temperature. Can. J. Bot. 45:537-541.
6. Gregory, P. H. 1968. Interpreting plant disease dispersal gradients. Annu. Rev. Phytopathol. 6:189-212.
7. Kampmeijer, P., and Zadoks, J. C. 1977. EPIMUL, a simulator of foci and epidemics in mixtures, multilines, and mosaics of resistant and susceptible plants. Simul. Monogr. Pudoc, Wageningen. 50 pp.
8. Kato, H., and Kozaka, T. 1974. Effect of temperature on lesion enlargement and sporulation of *Pyricularia oryzae* in rice leaves. Phytopathology 64:828-830.
9. Kermack, W. D., and McKendrick, A. G. 1927. A contribution to the mathematical theory of epidemics. Proc. R. Soc. London Ser. A 115:700-721.
10. Kiyosawa, S., and Shiyomi, M. 1972. A theoretical evaluation of the effect of mixed resistant variety with susceptible variety for controlling plant disease. Nippon Shokubutsu Byori Gakkaiho 38:41-51.
11. Lipps, P. E. 1980. The influence of temperature and water potential on asexual reproduction by *Pythium* spp. associated with slow rot of wheat. Phytopathology 70:794-797.
12. MacKenzie, D. R. 1976. Applications of two epidemiological models for the identification of slow stem rusting in wheat. Phytopathology 66:55-59.
13. MacKenzie, D. R. 1979. The multiline approach to the control of some cereal diseases. Pages 199-216 in: Proceedings of the Rice Blast Workshop. Int. Rice Res. Inst., Los Baños, Laguna, Philippines.
14. MacKenzie, D. R., and Villareal, R. L. 1976. The spread of rice blast disease. (Abstr.) Proc. Am. Phytopathol. Soc. 3:309.
15. Mehta, Y. R., and Zadoks, J. C. 1970. Uredospore production and

sporulation period of *Puccinia recondita* f. sp. *triticina* on primary leaves of wheat. Neth. J. Plant Pathol. 76:267-276.
16. Metz, J. A. J. 1978. The epidemic in a closed population with all susceptibles equally vulnerable; some results for large susceptible populations and small initial infections. Acta Biotheor. 27:75-123.
17. Minogue, K. P., and Fry, W. E. 1983. Models for the spread of disease: Model description. Phytopathology 73:1168-1173.
18. Rijsdijk, F. H., and Rappoldt, K. 1979. A model of spore dispersal inside and above canopies. Pages 407-410 in: Proc. Int. Conf. Aerobiol. 1st. Fed. Environ. Agency, ed. Ber. 5/79 Umwelt Bundes Amt, Berlin. 471 pp.
19. Thieme, H. R. 1977. A model for the spatial spread of an epidemic. J. Math. Biol. 4:337-351.
20. Thieme, H. R. 1979. Asymptotic estimates of the solutions of nonlinear integral equations and asymptotic speeds for the spread of populations. J. Reine Angew. Math. 306:94-121.
21. van den Bosch, F., Zadoks, J. C., and Metz, J. A. J. 1988. Focus expansion in plant disease. I: The constant rate of focus expansion. Phytopathology 78:54-58.
22. Vanderplank, J. E. 1960. Analysis of epidemics. Pages 230-289 in: Plant Pathology, an Advanced Treatise. Vol. 3. The Diseased Population: Epidemics and Control. J. G. Horsfall and A. E. Dimond, eds. Academic Press, New York.
23. Vanderplank, J. E. 1963. Plant Diseases: Epidemics and Control. Academic Press, New York. 349 pp.
24. Vanderplank, J. E. 1975. Principles of Plant Infection. Academic Press, New York. 216 pp.
25. Waggoner, P. E. 1952. Distribution of potato late blight around inoculum sources. Phytopathology 42:323-328.
26. Williams, E. J. 1961. The distribution of larvae of randomly moving insects. Aust. J. Biol. Sci. 14:598-604.
27. Zadoks, J. C. 1961. Yellow rust on wheat. Studies in epidemiology and physiologic specialization. Neth. J. Plant Pathol. 67:69-256.
28. Zadoks, J. C., and Kampmeijer, P. 1977. The role of crop populations and their deployment, illustrated by means of a simulator Epimul 76. Ann. N. Y. Acad. Sci. 287:164-190.